Agronomy Research **14**(S1), 1004–1014, 2016

Determination of the heat flux of steel for the heat treatment model of agricultural tools

A. Kešner[1,*], R. Chotěborský[1] and M. Linda[2]

[1]Department of Material Science and Manufacturing Technology Faculty of Engineering, Czech University of Life Sciences Prague, Kamýcká 129, CZ 165 21 Prague – Suchdol, Czech Republic
[2]Department of Electrical Engineering and Automation, Faculty of Engineering, Czech University of Life Sciences Prague, Kamýcká 129, CZ 165 21 Prague – Suchdol, Czech Republic;
[*]Correspondence: kesner@tf.czu.cz

Abstract. Chisels and tines for agricultural machinery are mechanically worn. Mechanical wear depends on the microstructure of the material. The desired microstructure of the material, specifically steel is obtained by heat treatment. Microstructure after heat treatment can be determined in two ways. The first one is the experimental determination, which is time-consuming and not economically efficient. The second is to build the thermal model during the heat treatment. Microstructure is affected during the heat flux during heat treatment. This research was focused on the boundary conditions of the model heat flux during quenching. The heat flux was measured during quenching with solid cylindrical samples (ø25–50 mm) by means of two thermocouples. The first temperature was measured in the axis of the sample and the second temperature was measured near the sample surface. The results of the heat flux were appointed to the model and experimentally verified. In this way it is possible to construct a model of tines and chisels for agricultural machine, which shows the progress of the heat flux during quenching.

Key word: quenching, FEM, tool steel, heat flux.

INTRODUCTION

Mechanical properties of the surface of a product are designed microstructure (Prabhu & Prasad, 2003; Li & Wells, 2005). For this reason an estimation of the hardening course is very important (Telejko, 2004). The most important step during quenching is cooling (Li & Wells, 2005). Quenching of steel in liquid medium consists of three distinct stages of cooling: vapor phase, nucleate boiling, and convective stage. In the first stage, a vapor blanket is formed immediately upon quenching. This blanket has an insulating effect and heat transfer in this stage is slow, since it is mostly through radiation (Prabhu & Prasad, 2003; Fernandes & Prabhu, 2007). The heat flux between the surface material and the hardening medium is essential to simulate hardening. The parameters affecting the heat flux are heating temperature, the sample surface, the movement of quenching media, thermo-physical properties of the sample and quenching media. The most widely used quenching medium is readily available and cheap water. The thermophysical properties of the water also depend on the correct setting of

boundary conditions of modeling to estimate the heat flux. The choosing exact boundary conditions allows the correct choice of quenching medium (Prabhu & Prasad, 2003; Li & Wells, 2005).

Estimation of the heat flux and the heat transfer coefficient of measured temperatures is based on the inversion method (Archambault et al., 1997; Babu & Prasanna Kumar, 2009; 2014). The right method for getting the realistic metal/quenchant interfacial heat transfer properties is inverse modeling and this method allows the determination of boundary conditions by the coupling of numerical methods with simple temperature measurements inside the quench probe (Prabhu & Prasad, 2003). The inverse method consists in numeric selection of boundary heat transfer conditions providing a heat distribution in the sensor not differing, within the necessary accuracy limits, from the assumed one (Buczek & Telejko, 2004; Lu et al., 2013). Various ways of inverse method solutions are documented (Ref.). Heat flux transient technique was found to be more accurate than the Grossmann technique in assessing the severity of quenching (Prabhu & Prasad, 2003). Telejko (Telejko, 2004) applied the method of inverse thermal conductivity. Thermal conductivity computations were done using measured temperature profiles. Heat equations were compiled using the finite element method (FEM). The optimization computing has been solved by the Broyden–Fletcher–Goldfarb–Shanno (BFGS) variable metric method. (Ramesh & Narayan Prabhu, 2014) used a high performance smart camera for temperature measurement. Specifications of these methods are described for example in (Blackwell & Beck, 2010), wherein the model equation are parabolic in time, provided that the heat flux is constant over time. The predicted temperature is used to reduce errors in the estimates of heat flux measurements and also to stabilize the calculation as the time steps. The heat flux is determined so as to minimize the least squares error between the model and experimental temperatures and it is also thoroughly monitored during casting. Methods of detection also include using a 3-D inversion technique. For best detection of the temperature course thermocouples are placed in transverse and longitudinal sections, which also serve as input parameters to boundary conditions (Hebi et al., 2006).

For accurate simulation of heat treatment it is necessary to accurately estimate temperatures in the components and know the thermo-physical properties and quenching media (Archambault et al., 1997; Telejko, 2004). To predict the temperature field of the heat treatment finite element models were developed. Thermal conductivity λ can be calculated if the density ρ and specific heat capacity c_p are known (Telejko, 2004).

Babu (Babu & Prasanna Kumar, 2009) proposed description of heat flux as a function of dimensionless parameters. Boundary conditions were set in ANSYS. Their results showed that the heat flux is dependent on the initial heating temperature.

High-current cooling of the material has been shown to provide big temperature differences in the material and correct mathematical model makes it possible for it to be preceded by deformation of the material (Naceur et al., 2011). Accuracy of the FEM facilitated successful comparison of two cooling media (Buczek & Telejko, 2013).

Hardening of the material creates bainitic or martensitic structure (Fernandes & Prabhu, 2007). When creating heat equations, it is necessary to take into account the phase transformation during quenching (Telejko, 2004). Correct estimate of the course of heat treatment can predict the course of phase transformations (Babu & Prasanna Kumar, 2014).

(Prabhu & Fernandes, 2007) discovered that the surface roughness of the product has a significant effect on the flow of the thermal field and thus the final microstructure component. Grooved surface had fully martensitic structure. Smooth surface had a mixed microstructure.

The phase transformations occur during the hardening of the material. (Hernandez-Morales et al., 1992), like most authors in literature, phase transformation during heat flux is neglected. (Telejko, 2004) summed knowns temperature phase transformations and calculations divided into three steps. In the first step calculations the thermal conductivity up to temperature of phase transformation is determined on the basis of a heating test. In the second step, function for the temperatures above the phase transformation is calculated by using the temperature measurements from the cooling test. Finally, the thermal conductivity was determined using all the temperatures.

The sets of boundary conditions are crucial to model accuracy. It is necessary to use algorithm to optimization of heat treatment which their aim will be found to thermal cycle to ideal structure. The algorithm of FEM model needs a general model for a sets of Neumann conditions. Other than simple function to FEM programming increase the time calculation. Thus losing the advantage of modeling. Generalized functions can be used for creating FEM models. This function can be used, for example, to optimization of heat treatment of agricultural tools (Chotěborský & Linda, 2015).

This paper is focused onto estimate of simple equation of heat flux during quenching at different conditions of cooling and heating temperatures. The simple nonlinear function is generalized to set temperature conditions.

MATERIAL AND METHODS

The method in this work enables estimation of the heat flux on the basis of the inverse method using the FEM model. Chemical composition of tested steel is presented in Table 1.

Table 1. Chemical composition of steel 25CrMo4 in wt. %

	C	Mn	Si	P	S	Cr	Ni	Mo	Cu	V
25CrMo4	0.250	0.710	0.230	0.018	0.022	1.030	0.090	0.210	0.230	0.004

The experimental procedure consisted of a furnace for heating the samples. A container with water as cooling media was placed next to the furnace for quick transfer of samples into the bath. Eighteen samples (ø25–50mm) were used each to which was secured a pair of thermocouples (near the surface and the axis of the sample). Thermocouples were electrically isolated with a protective coating and connected to the measuring apparatus. The measuring apparatus was connected to the computer and measured temperatures were recorded during the heat treatment. The experimental system is shown in Fig. 1.

Quenching had different heating temperatures (800 °C, 900 °C and 1,000 °C), and done in a calm cooling environment (standing water) or a moving cooling medium (turbulent water). Heating holding time was 0.5 hours for each sample. Each measurement was repeated 3 times at the heating temperature (It was processed a total of 18 samples).

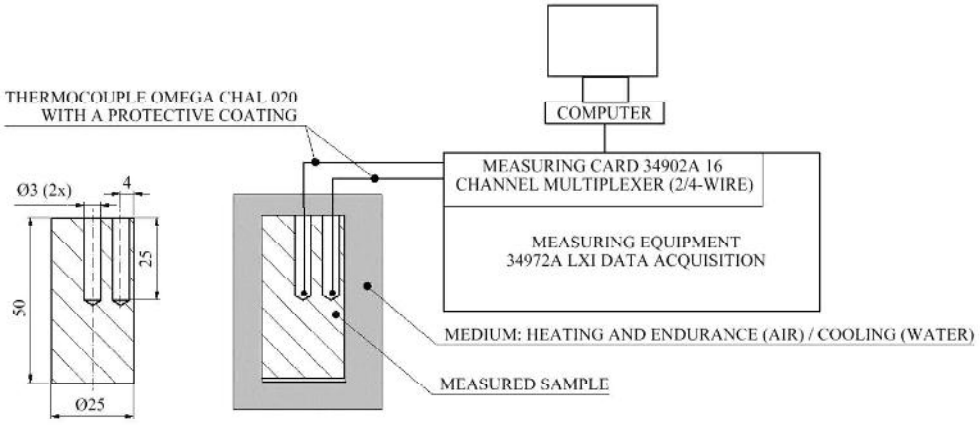

Figure 1. Scheme of measurements of heat treatment of samples.

The recorded measure data (time, temperature) were separated to a heating, holding time at heating temperature and the cooling stage. These two steps were separated by an algorithm written in SCILAB 5.5.1 – See Fig. 2.

From the cooling were obtained temperature differences of surface and core of sample. Furthermore, according to the eqn 1, absolute temperatures were transformed to the relative temperatures (dimensionless temperature-from 0 to 1).

$$r = \frac{T_K - T_{MINK}}{T_{MAXK} - T_{MINK}} (-) \tag{1}$$

where: T_K – actual surface temperature (K); T_{MINK} – minimum surface temperature (K); T_{MAXK} – maximum surface temperature (K).

Experimental heat flux was calculated from eqn 2:

$$q = \pi \cdot \lambda \cdot \frac{\Delta T}{rt} \tag{2}$$

where: q – heat flux (W m^{-2}); λ – thermal conductivity (W m^{-1} K^{-1}); ΔT – difference the measured temperature on surface and in the core of sample (K); rt – the measured distance of thermocouples (m).

The constants c_0, c_1, c_2 were determined by Levenberg-Marquardt algorithm according to eqn. 3 and 4. The constants c_1, c_2 characterize curve slope.

$$fce(r) = c_0 \cdot r^{c_1} \cdot (1 - r)^{c_2} \tag{3}$$

where: c_o – constant (boost) (-); c_1, c_2 – constants (slope from the peak) (-).

$$\sum_{i=1}^{n-1} \left(\Delta T_i \cdot (x_i - x_{i+1})\right) = \int_0^1 fce(r) \tag{4}$$

where: ΔT_i – difference of the cooling temperature at time (K); x_i – the absolute value of the axis x (-).

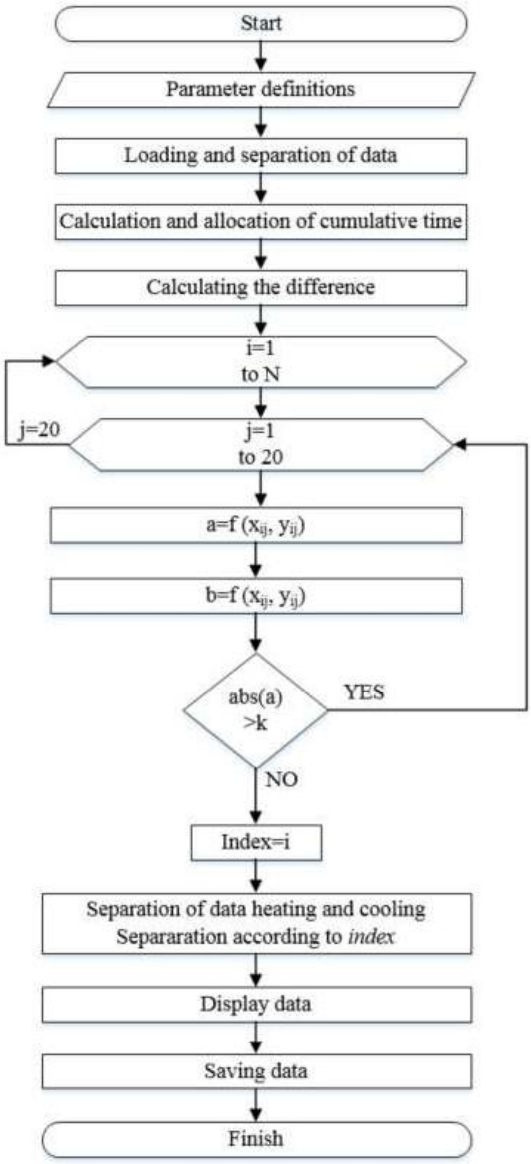

Figure 2. Flow chart for data processing, where N is number of measured data, j = 20 is set number of data for regression (fixed number of data for regression with regard to the course of the derivation measurement data – the result was affected at smaller value), a and b are the parameters functional dependency f(x) = ax+b, k is set directive for compared to with the calculated value.

These values have been transformed from relative values into absolute values for the FEM calculation using eqn 5.

$$x_i = r \cdot (T_{MAX} - x_0) + x_0 \quad (5)$$

where: x_0 – the surface temperature during cooling (K).

The course of the calculated heat flux depending on the calculated surface temperature is shown in Fig. 5. Calculated surface temperature was calculated from eqn 6.

$$\mathrm{Tpc} = \frac{\mathrm{r}^2 \cdot (\mathrm{Tp} - \mathrm{Ta})}{\mathrm{rt}^2} + \mathrm{Ta} \tag{6}$$

where: r – the radius of the sample (m); Tp – measured surface temperature (K); Ta – measured core temperature (K).

RESULTS AND DISCUSSION

Measured data of surface and core temperatures of samples were used to fit Eqn (2). The result is shown in Fig. 3. It is dependency between heat flux and dimensionless temperature for sample 25CrMo4 number 1 – cooled in calm waters at 800 °C heating temperature.

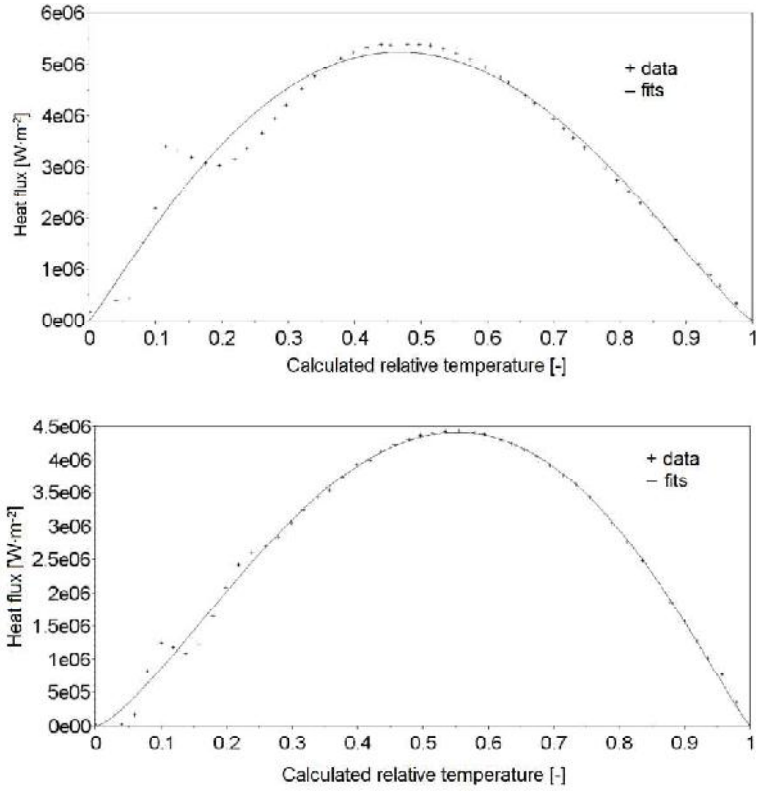

Figure 3. Dependency between heat flux and relative temperature – in the upper part is sample 25CrMo4 number 1 – cooled in calm waters at temperature of heating 800 °C and in down part is sample 25CrMo4 number 14 – cooled in calm waters at temperature of heating 1,000 °C.

In Figs 3–6 are shown dependency between coefficients c_0, c_1, c_2 and temperature of the heating furnace. The results show that a correlation exists between these coefficients and heating temperature. In Figs 3–6 are presented obtained coefficient from fit and heating temperatures. Obtained data can be fitted by regression, index of determination show a significant and close correlation between coefficients and heating temperature. Increasing heating temperature was observed to influence coefficients of Eqn. 3. Dependency between coefficients and heating temperature show decreasing character.

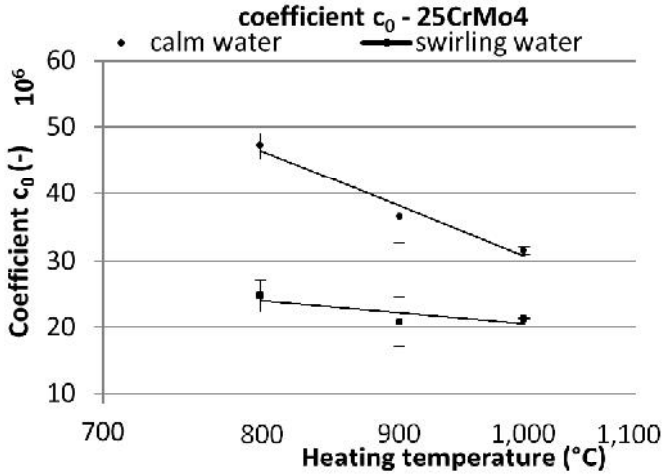

Figure 4. Dependency between coefficient c_0 and heating temperature for steel 25CrMo4.

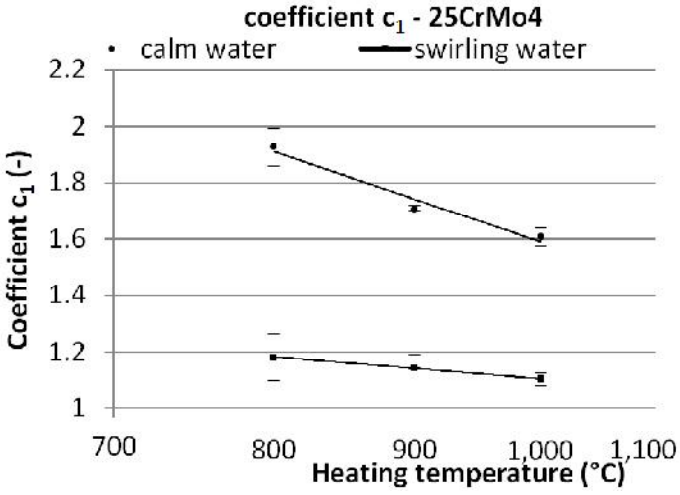

Figure 5. Dependency between coefficient c_1 and heating temperature for steel 25CrMo4.

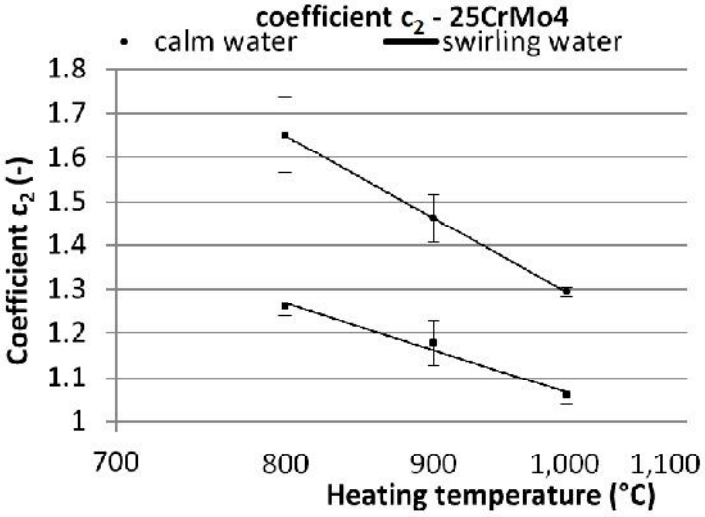

Figure 6. Dependency between coefficient c_2 and heating temperature for steel 25CrMo4 number 12 – cooled in calm waters at various heating temperature.

Eqn. 3 can be generalized if we use a temperature dependency of coefficient these equation according to regression function (Table 2). In Table 3 are presented correlation between mathematical models according to Eqn. 3. Statistical analysis show that the mathematical model is close to measured data and it can be used as a general model in the 800–1,000 °C temperature range.

Table 2. Temperature dependency of coefficient according to regression function

coefficients	calm water	swirling water
c_0	$7{,}030 \times 10^{-7} \cdot \log(T) + 5{,}164 \cdot 10^{8}$	$1{,}545 \times 10^{-7} \cdot \log(T) + 1{,}273 \cdot 10^{8}$
c_1	$-1.433 \cdot \log(T) + 11.491$	$-0.357 \cdot \log(T) + 3.566$
c_2	$-1.605 \cdot \log(T) + 12.377$	$-0.902 \cdot \log(T) + 7.299$

Table 3. Correlation between mathematical model and measured data

	800 °C	900 °C	1,000 °C
calm water	0.996118	0.983460	0.995671
swirling water	0.991619	0.990898	0.992837

Correlation between mathematical model and measured data was calculated according to Eqn. 7 (Xu et al., 2016)

$$r_{xy} = \frac{n \cdot \sum x_i.y_i - \sum x_i \cdot \sum y_i}{\sqrt{n \cdot \sum x_i^2 - (\sum x_i)^2} \cdot \sqrt{n \cdot \sum y_i^2 - (\sum y_i)^2}} \tag{7}$$

where: x are measured data (°C); y are calculated data (°C); n is number of data (pcs).

Fig. 7 shows dependency between predicted heat flux and measurement heat flux.

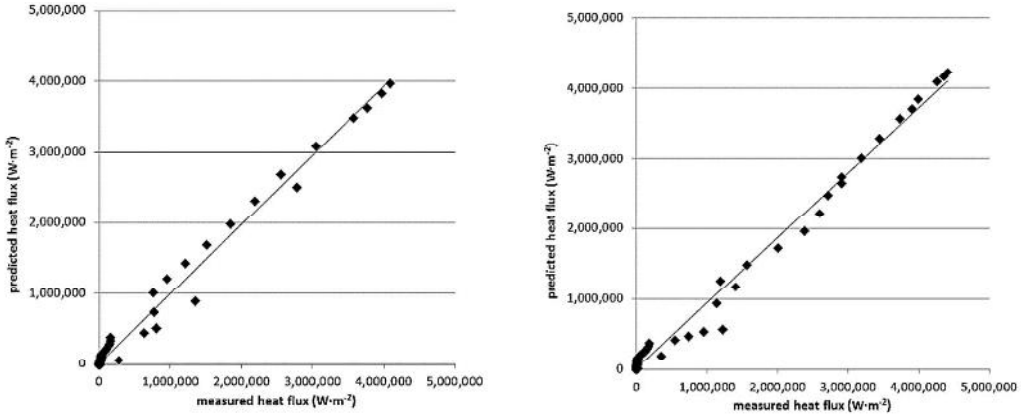

Figure 7. Dependancy between predicted heat flux and measurement heat flux – left side for sample 1 and right side for sample 14.

(Prabhu & Prasad, 2003; Li & Wells, 2005; Abishek et al., 2013;) in their articles performed similar measurements at a single heating temperature. In this study, there were three heating temperature which led to a refinement of the model.

(Prabhu & Fernandes, 2007; Babu & Prasanna Kumar, 2009; Babu & Prasanna Kumar, 2014;) in their publications took same measurements under various cooling environments and the dependencies of heat flux were described using polynomial functions. If we look at the value of function near the boundary conditions (near to maximal and minimal temperatures), polynomial function can yield fatal errors near the boundary conditions. The function presented in this article eliminates those errors and it can be generalized. The polynomial function on the other hand cannot be generalized.

For the present model, it is not necessary do experimental validation of heat fluxes at temperatures other than those listed in this article. It is possible to construct algorithms for finding optimal heat treatment parameters in order to reduce the energy and time consumption in production while maintaining or improving the mechanical properties of agricultural tools.

CONCLUSIONS

The following findings can be summarized from the experimental measurements:

- depending on the surface temperature, the position of the maximum flux rises with increasing heating temperature;
- there is a link between the coefficients c0, c1 and c2 eqn 2 and the heating temperature;
- function in this article eliminates physical errors, unlike commonly used polynomial function;
- the outcrop function of this study can be generalized;

- the process of creating FEM models used in this article enables design heat treatment without verification with the experimental treatment with different temperatures than those mentioned in this article;
- algorithms for finding optimal heat treatment parameters – while reducing energy and time consumption and maintaining or improving the mechanical properties of agricultural tools can be created for the procedure above.

ACKNOWLEDGEMENT. Supported by Internal grant 31140/1312/3105 agency of Faculty of Engineering, Czech University of Life Sciences in Prague.

REFERENCES

Abishek, S., Narayanaswamy, R. & Narayanan, V. 2013. Effect of heater size and Reynolds number on the partitioning of surface heat flux in subcooled jet impingement boiling. *International Journal of Heat and Mass Transfer* **59**, 247–261.

Archambault, P., Denis, S. & Azim, A. 1997. Inverse resolution of the heat-transfer equation with internal heat source: Application to the quenching of steels with phase transformations. *Journal of Materials Engineering and Performance* **6**(2), 240–246.

Babu, K. & Prasanna Kumar, T.S. 2009. Mathematical Modeling of Surface Heat Flux During Quenching. *Metallurgical and Materials Transactions B* **41**(1), 214–224.

Babu, K. & Prasanna Kumar, T.S. 2014. Comparison of Austenite Decomposition Models During Finite Element Simulation of Water Quenching and Air Cooling of AISI 4140 Steel. *Metallurgical and Materials Transactions B* **45**(4), 1530–1544.

Blackwell, B. & Beck, J.V. 2010. A technique for uncertainty analysis for inverse heat conduction problems. *International Journal of Heat and Mass Transfer* **53**(4), 753–759.

Buczek, A. & Telejko, T. 2004. Inverse determination of boundary conditions during boiling water heat transfer in quenching operation. *Journal of Materials Processing Technology* **155-156**, 1324–1329.

Buczek, A. & Telejko, T. 2013. Investigation of heat transfer coefficient during quenching in various cooling agents. *International Journal of Heat and Fluid Flow* **44**, 358–364.

Fernandes, P. & Prabhu, K.N. 2007. Effect of section size and agitation on heat transfer during quenching of AISI 1040 steel. *Journal of Materials Processing Technology* **183**(1), 1–5.

Hebi, Y., Man, Y. & Dacheng, F. 2006. 3-D Inverse Problem Continuous Model for Thermal Behavior of Mould Process Based on the Temperature Measurements in Plant Trial. *ISIJ International* **46**(4), 539–545.

Hernandez-Morales, B., Brimacombe, J.K. & Hawbolt, E.B. 1992. Application of inverse techniques to determine heat- transfer coefficients in heat- treating operations. *Journal of Materials Engineering and Performance* **1**(6), 763–771.

Chotěborský, R. & Linda, M. 2015. FEM based numerical simulation for heat treatment of the agricultural tools. *Agronomy Research* **13**(3), 629–638.

Li, D.I. & Wells, M.A. 2005. Effect of subsurface thermocouple installation on the discrepancy of the measured thermal history and predicted surface heat flux during a quench operation. *Metallurgical and Materials Transactions B* **36**(3), 343–354.

Lu, J.F., Bourouga, B. & Ding, J. 2013. Transient boiling heat transfer performances of subcooled water during quenching process. *International Communications in Heat and Mass Transfer* **48**, 15–21.

Naceur, I.B., Kchaou, M. & Ksibi, H. 2011. Optimization of local cooling for hot components by a water jet. *Metal Science and Heat Treatment* **53**(5–6), 233–238.

Prabhu, K.N. & Fernandes, P. 2007. Effect of surface roughness on metal/quenchant interfacial heat transfer and evolution of microstructure. *Materials & Design* **28**(2), 544–550.

Prabhu, K.N. & Prasad, A. 2003. Metal/Quenchant Interfacial Heat Flux Transients During Quenching in Conventional Quench Media and Vegetable Oils. *Journal of Materials Engineering and Performance* **12**(1), 48–55.

Ramesh, G. & Narayan Prabhu, K. 2014. Spatial Dependence of Heat Flux Transients and Wetting Behavior During Immersion Quenching of Inconel 600 Probe in Brine and Polymer Media. *Metallurgical and Materials Transactions B* **45**(4), 1355–1369.

Telejko, T. 2004. Analysis of an inverse method of simultaneous determination of thermal conductivity and heat of phase transformation in steels. *Journal of Materials Processing Technology* **155-156**, 1317–1323.

Telejko, T. 2004. Application of an inverse solution to the thermal conductivity identification using the finite element method. *Journal of Materials Processing Technology*.

Xu, W., Ma, R., Zhou, Y., Peng, S. & Hou, Y. 2016. Asymptotic properties of Pearson′s rank-variate correlation coefficient in bivariate normal model. *Signal Processing* **119**, 190–202.